

Received: 2017.10.04  
Accepted: 2017.11.27  
Published: 2017.12.26

# Pioglitazone Attenuates Atherosclerosis in Diabetic Mice by Inhibition of Receptor for Advanced Glycation End-Product (RAGE) Signaling

Authors' Contribution:  
Study Design A  
Data Collection B  
Statistical Analysis C  
Data Interpretation D  
Manuscript Preparation E  
Literature Search F  
Funds Collection G

ACEF 1 **Hongli Gao**  
ABG 1,2 **Hongwei Li**  
BCD 1,2 **Weiping Li**  
BDF 1 **Xuhua Shen**  
BCF 1 **Beibing Di**

1 Cardiovascular Center, Beijing Friendship Hospital, Capital Medical University, Beijing, P.R. China  
2 Beijing Key Laboratory of Metabolic Disorders Related Cardiovascular Disease, Beijing, P.R. China

**Corresponding Authors:** Hongwei Li, e-mail: [lh19656@sina.com](mailto:lh19656@sina.com)

**Source of support:** This work was supported by a grant from the National Natural Science Foundation of China (No. 81670315)

**Background:** Peroxisome proliferator-activated receptor- $\gamma$  (PPAR- $\gamma$ ) exhibits anti-inflammatory and anti-diabetic properties, and is protective against cardiovascular diseases. This study aimed to determine the effects of a PPAR- $\gamma$  agonist pioglitazone on atherogenesis in an ApoE knockout mouse (ApoE<sup>-/-</sup>) diabetic mouse model and in a cultured vascular smooth muscle cells (VSMCs) model.

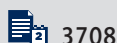
**Material/Methods:** Male ApoE<sup>-/-</sup> mice were rendered diabetic by 5 daily intraperitoneal injections of streptozotocin. Pioglitazone (20 mg/kg/d) or PPAR- $\gamma$  inhibitor GW9662 (1 mg/kg/d) were administered for 12 weeks. At the end of treatment, mice were killed and the aortae were isolated. Oil Red O staining was used to evaluate atherosclerotic plaque area. H&E staining was used to evaluate the number of complicated plaques. Western blotting and immunohistochemistry were used to determine the expression of advanced glycation end-products (RAGE) and PPAR- $\gamma$ . The effects of pioglitazone and GW9662 on RAGE and PPAR- $\gamma$  expression were examined in cultured primary mouse VSMCs in hyperglycemic conditions.

**Results:** Administration of pioglitazone in diabetic ApoE<sup>-/-</sup> mice successfully reduced atherosclerotic plaque area and the number of complicated plaques. Moreover, pioglitazone inhibited RAGE and stimulated PPAR- $\gamma$  protein expression in atherosclerotic plaques of diabetic ApoE<sup>-/-</sup> mice. In cultured VSMCs upon high-glucose challenge, pioglitazone downregulated RAGE mRNA and protein expression. Blockade of PPAR- $\gamma$  activity by GW9662 remarkably attenuated the inhibitory actions of pioglitazone on atherogenesis, both in diabetic ApoE<sup>-/-</sup> mice and in cultured VSMCs, upon high-glucose challenge.

**Conclusions:** Pioglitazone has a therapeutic effect on atherosclerosis in diabetes, and inhibition of RAGE signaling plays a critical role in mediating the beneficial effects of pioglitazone.

**MeSH Keywords:** **Atherosclerosis • Diabetes Mellitus • Muscle, Smooth, Vascular**

**Full-text PDF:** <https://www.medscimonit.com/abstract/index/idArt/907401>



## Background

Many clinical observational studies in prospective cohorts have found patients with diabetes to have a greater risk, nearly 2 to 6 times that among persons without diabetes, of morbidity and mortality from cardiovascular disease [1,2]. Macrovascular complications of diabetes mellitus, such as stroke and coronary heart disease (CHD), account for more than 50% of deaths in people with diabetes and incur considerable social and economic burden [3]. Currently, there is widespread acceptance that aggravated macrovascular complications in patients with diabetes are associated with the accelerated development and progression of atherosclerosis [4]. Metabolic and hemodynamic factors such as hyperglycemia, hyperlipidemia, and hypertension contribute to components of vascular injury such as endothelial dysfunction and vascular smooth muscle cell (VSMC) apoptosis, and thereby contribute to the pathogenesis and progression of diabetes-associated atherosclerotic lesions [5]. An emerging view is that the onset of diabetes-associated vascular injury precedes a formal diagnosis of diabetes [6]. These considerations highlight the concept that vascular injury accelerates atherosclerosis and leads to diabetes-associated atherosclerosis; therefore, research insights are essential for optimal management to prevent diabetic macrovascular disease.

Pioglitazone is a member of the thiazolidinedione (TZD) family of glucose-lowering agents that stimulate the peroxisome proliferator-activated receptor-gamma (PPAR- $\gamma$ ), and it is widely prescribed for the treatment of type 2 diabetes (T2D). Compared with rosiglitazone, another TZD, which was withdrawn from some markets after concerns about an increased risk of cardiac events, current clinical data indicate that pioglitazone is an effective and well-tolerated agent for use in patients with T2D [7]. For example, pioglitazone decreased coronary artery inflammation in patients with impaired glucose tolerance or diabetes in a mechanism independent of blood glucose reduction [8]. In patients with T2D, pioglitazone increased myocardial glucose uptake, improved the early peak flow rate and left ventricular compliance, and reduced hepatic triglyceride content, suggesting that pioglitazone is associated with improvement in cardiac function and whole-body insulin sensitivity [9]. Further, a systematic review and meta-analysis showed that pioglitazone treatment in stroke patients with insulin resistance, prediabetes, and diabetes mellitus reduced the risk of recurrent stroke and future major vascular events [10]. Importantly, a great number of clinical investigations in patients with diabetes have revealed that pioglitazone has a protective effect against atherosclerosis by lowering the triglyceride/high-density lipoprotein cholesterol ratio [11], attenuating plaque inflammation [12], and increasing particle size or decreasing particle concentration [13]. Nevertheless, the underlying molecular mechanisms of the protective effect of pioglitazone against atherosclerosis are still largely unknown.

The receptor for advanced glycation end-products (RAGE) is a 35-kDa transmembrane receptor of the immunoglobulin superfamily that was first characterized in 1992 [14]. Accumulating evidence from both clinical and preclinical studies demonstrates that RAGE plays a central role in inflammation. Activation of intracellular RAGE in the endothelium, mononuclear phagocytes, or lymphocytes triggers key proinflammatory mediators, and blockade of RAGE signaling delayed hypersensitivity and inflammatory colitis in murine models [15]. Moreover, RAGE mediates the advanced glycation end-products (AGEs)-induced adhesion of polymorphonuclear leukocytes to endothelial cells [16]. Importantly, Bucciarelli et al. showed that blockade of RAGE stabilizes atherosclerosis and vascular inflammation in murine diabetic model [6]. In humans, RAGE overexpression in plaque macrophages is shown to be associated with enhanced inflammatory reaction, and contributes to plaque destabilization by inducing culprit metalloproteinase expression [17].

In the present study, we hypothesized that pioglitazone protects against atherosclerosis by modulation of RAGE signaling. The potential effects of pioglitazone on atherosclerosis and RAGE signaling were examined in both an ApoE<sup>-/-</sup> diabetic mice model and a cultured vascular smooth muscle cell (VSMC) model.

## Material and Methods

### Animals

Male 6-week-old C57BL/6 mice and ApoE knockout mice were purchased from Beijing Vital River Laboratory Animal Technology Co., Ltd. (Beijing, China) and housed at the animal facility of Capital Medical University, China. The mice were maintained on a 12-h light–dark cycle and stable environmental temperature (23°C) in a pathogen-free environment with free access to chow and water. The protocol for the animal study was approved by the Animal Research Ethics Committee of Capital Medical University, China. Animals were used in accordance with our institutional guidelines for animal care.

### Animal model procedure

The diabetic atherosclerosis animal model in ApoE-knockout (ApoE<sup>-/-</sup>) mice was produced according to a method from a previous study, but with modifications [18]. At 6 weeks of age, some ApoE<sup>-/-</sup> mice were rendered diabetic by administration of 5 daily intraperitoneal injections of streptozotocin (60 mg/kg; Sigma-Aldrich St. Louis, MO, USA) in citrate buffer (0.05 mol/L; pH 4.5). Control ApoE<sup>-/-</sup> mice were similarly treated with citrate buffer only (Control group). Serum glucose was measured from tail vein blood using a glucometer 1 week later. Only the streptozotocin-injected mice with serum glucose >16.7 mmol/L were considered to be diabetic and were

divided into 3 groups: diabetes group (D group), diabetes + pioglitazone group (D + P group), and diabetes + pioglitazone + GW9662 group (D + P + G group). Mice of the D + P group received pioglitazone (20 mg/kg/d) by gavage, whereas mice of the D + P + G group were given pioglitazone (20 mg/kg/d) by gavage and received an intraperitoneal injection of GW9662 (1 mg/kg/d). Normal ApoE<sup>-/-</sup> mice (without diabetes; Control group) and diabetic ApoE<sup>-/-</sup> mice (D group) were administered the same volume of saline by the same route. Treatment administration was continued for 12 weeks, after which the mice were sacrificed at 20 weeks of age.

### Tissue sampling

Mice were anesthetized by an intraperitoneal injection of 10% chloral hydrate (400 mg/kg) and the abdomen of each mouse was opened along the greater curvature for examination of the aorta. Then, the mouse was perfused with phosphate-buffered saline (PBS; 0.01 M) for 10 min through the heart to flush the blood from the vasculature. In experiments for Western blotting analysis, the aortae were dissected swiftly in this liquid ammonia and stored at -80°C. In another set of experiments for Oil Red O, immunohistochemistry, and hematoxylin & eosin (H & E) staining, aortae were isolated after an additional perfusion with 4% paraformaldehyde for 15 min.

### Oil Red O staining

To analyze atherosclerotic lesions, Oil Red O staining was applied. The whole aortae were cut into 3 portions: aortic arch, thoracic aorta, and abdominal aorta. The luminal aspect of the aorta was opened and stained with Oil Red O as described previously [19]. The Oil Red O (#O0625) was purchased from Sigma-Aldrich (St. Louis, MO, USA). To prepare a stock Oil Red O staining solution, 0.5 g Oil Red O was dissolved in 100 mL isopropanol and heated in a water bath, filtered, and stored at 4°C. During staining, the aortae were rinsed with 60% isopropanol for 1 min, stained with a freshly prepared Oil Red O working solution for 15 min, rinsed with 60% isopropanol again, and washed with distilled water for 3 min before imaging. The Oil Red O-positive area (red) was regarded as fat deposit. For quantitative analysis, images of aortae were subjected to quantitative morphometry analysis using Image-Pro Plus (Media Cybernetics, Silver Spring, MD, USA). Proportions of Oil Red O-staining positive lesions in the aortic arch, thoracic aorta, abdominal aorta, and whole aorta were calculated.

### Histology and immunohistochemistry

After perfusion with 4% paraformaldehyde solution for 15 min, aortae dissected from mice were fixed in 4% paraformaldehyde solution for an additional 24 h. Then, they were processed into paraffin blocks, cut into 6- $\mu$ m-thick cross-sections, and

subjected to H & E staining, as described previously, to determine the presence of complicated plaques [20]. If there was rupture or fracture of the fibrous cap of the fibrous plaque, hemorrhage into the plaque, mural thrombosis, or prominent fibrosis, the atherosclerotic plaques were classified as complicated plaques.

To determine the expression of RAGE and PPAR- $\gamma$  in atherosclerotic lesions, immunohistochemistry was performed as described previously [21,22]. Briefly, 6- $\mu$ m-thick tissue sections were blocked by 8% normal goat serum and incubated in specific primary antibodies targeting RAGE (#3611, Abcam, Cambridge, MA, USA) and PPAR- $\gamma$  (#45036, Abcam, Cambridge, MA, USA), respectively, overnight at 4°C. Then, the sections were washed 3 times in PBS times and incubated with corresponding biotin-conjugated secondary antibodies (Rockland Immunochemicals, Gilbertsville, PA, USA) for 2 h. Again, after being washed 3 times by PBS, the sections were incubated with horseradish peroxidase (HRP)-streptavidin for 30 min at 37°C. A solution of diaminobenzidine was applied onto the sections for visualizing immunoreactivity; brown areas indicated positive staining. Stained specimens were mounted on glass slides and examined under a BX 41 Olympus microscope to obtain images, which were analyzed using Image-Pro Plus (Media Cybernetics, Silver Spring, MD, USA) to calculate integrated optical density (IOD). For each animal, at least 5 sections and at least 5 different visual fields in each section were recorded and evaluated in statistical analysis.

### Mouse VSMCs culture and treatment

Mouse VSMCs were isolated and cultured in accordance with a standard enzymatic digestion technique [23]. Animals were sacrificed with an injected overdose of intraperitoneal chloral hydrate. Thoracic and abdominal aorta were removed and placed in a dish filled with ice-cold D-Hank's solution and cleaned of perivascular adipose tissue and denuded of endothelium with forceps. Then, aortae were incubated with an enzymatic solution (2 mg/mL collagenase II, Sigma-Aldrich St. Louis, MO, USA) for 45 min. Aortae were transferred to a serum-free medium to remove the adventitia completely with a stereoscope, followed by immersion in 0.25 mg/mL elastase (Type III, Sigma-Aldrich St. Louis, MO, USA) for an additional 1 h. The endothelium was removed during the incubation with collagenase and elastase. The entire aortae disintegrated into single cells, and the digested aortae were transferred into a 50-mL conical tube and gently triturated with a glass pipette. After centrifugation at 800 g for 3 min, the supernatant was removed. Sedimented cells were resuspended in 2 mL Dulbecco's modified Eagle's medium (DMEM) supplemented with 10% fetal bovine serum in an incubator with 95% O<sub>2</sub> and 5% CO<sub>2</sub> as described previously [24]. Experiments were performed using cells between passages 3 and 8.

Before experiments, VSMCs were serum starved for 24 h, and the medium was replaced with a fresh one. Then, cells were divided into 5 groups as follows: (1) normal-glucose group (N group, 5.5 mmol/L glucose); (2) high-glucose group (G group, 25 mmol/L glucose); (3) high-glucose + pioglitazone group (G + P group, 25 mmol/L glucose + 10  $\mu$ mol/L pioglitazone); (4) high-glucose + pioglitazone + GW9662 group (G + P + W group, 25 mmol/L glucose + 10  $\mu$ mol/L pioglitazone + 10  $\mu$ mol/L GW9662); and (5) high-glucose + GW9662 group (G + W group, 25 mmol/L glucose + 10  $\mu$ mol/L GW9662). Cells were treated for 24 h, as described, and then subjected to real-time PCR and immunoblotting analyses.

### RNA extraction and real-time PCR

Total RNA was extracted from cells using TRIzol (Invitrogen, Carlsbad, CA, USA) according to the manufacturer's instructions. Reverse transcription was performed on 10 ng of total RNA with M-MLV reverse transcription (Promega, Madison, WI, USA). Quantitative real-time PCR was performed with a SYBR green PCR kit (Takara, Kyoto, Japan) in an ABI 7500 Real-time PCR system (ABI Biosystems, Perkin Elmer Applied Biosystems, Foster City, CA, USA). The following primers were used for real-time PCR analysis: RAGE: Forward, 5'-CTG GGT GCT TCT TGC T-3', Reverse, 5'-TCC CTC GCC TGT TAG TTG C-3'; PPAR- $\gamma$ : Forward, 5'-TTT TCA AGG GTG CCA GTT TC-3', Reverse, 5'-GGC TTC CGC AGG CTT TT-3'.  $\beta$ -Actin was used as an internal control. The primer for  $\beta$ -actin was as follows: Forward, 5'-GCT GTC CCT GTA TGC CTC TG-3', Reverse, 5'-TGT CAC GCA CGA TTT CCC T-3'. After amplification, a melting curve was acquired by heating the product at 20°C/s to 95°C, cooling it at 20°C/s to 55°C, keeping it at 55°C for 20 s, and then slowly heating it at 0.1°C/s to 94°C. Fluorescence was measured continuously during the slow temperature rise to monitor dissociation to assure product melting. The comparative analysis was performed by the  $2^{-\Delta\Delta Ct}$  method as described previously [24]. Each reaction was performed in triplicate.

### Western blotting analysis

Immunoblotting assays for expression of RAGE and PPAR- $\gamma$  were performed as described previously [25,26]. Cultured cells or aortic tissues were lysed by lysis buffer (50 mM Tris-Cl, 150 mM NaCl, 100  $\mu$ g/mL phenylmethylsulfonyl fluoride, 1  $\mu$ g/mL aprotinin, and 1% Triton X-100) with a protease inhibitors cocktail (1  $\mu$ g/mL leupeptin, 1  $\mu$ g/mL pepstatin, 20  $\mu$ g/mL phenyl methyl sulfoxide (PMSF), and 2  $\mu$ g/mL aprotinin). The homogenate was centrifuged at 12 000 rpm for 15 min. The supernatant was collected and the sediment was removed. Samples were boiled in 95°C with SDS-PAGE sample loading buffer for 10 min. Protein concentration was determined with a Bradford assay (Beyotime, Haimen, China) using bovine serum albumin as a standard reference. Approximately 30  $\mu$ g protein samples were loaded and run on SDS-polyacrylamide gels (10%). The gels were transferred to nitrocellulose membranes and

immunoblotting was performed as previously described. Briefly, the membranes were blocked by 10% goat serum and then incubated with primary antibodies (RAGE, 1: 2000; PPAR- $\gamma$ , 1: 1500; actin, 1: 3000) overnight at 4°C. After three 5-min washes in triethanolamine-buffered saline solution with Tween (TBS-T), the membranes were incubated with HRP-labeled secondary antibodies (1: 1, 000, Santa Cruz Biotechnology, CA, USA) for 4 h at room temperature. The membranes were then further washed by TBS-T solution 3 times. Protein bands were visualized by enhanced chemiluminescence (Arlington Heights, IL, USA). The optical density of bands was evaluated using Image J (NIH), and a statistical comparison was performed.

### Statistical analysis

SPSS 13.0 software (Chicago, Illinois, USA) was used for statistical analysis. All quantitative data were expressed as mean  $\pm$  standard deviation. Comparison between groups was done using one-way ANOVA test followed by post hoc test (least significant difference).  $p < 0.05$  was considered to indicate a statistically significant difference.

## Results

### Pioglitazone treatment reduces atherosclerotic lesion area in ApoE<sup>-/-</sup> diabetic mice

Oil Red O staining showed that the atherosclerotic lesion area in the aortic arch of ApoE<sup>-/-</sup> diabetic mice (D group) was higher than that in control ApoE<sup>-/-</sup> mice (C group,  $p=0.001$ , whereas the atherosclerotic lesion area in the D + P group was significantly reduced ( $p=0.001$ , Figure 1A), suggesting that pioglitazone treatment reduced the increase of atherosclerotic lesion area under diabetic conditions. Notably, the proportion of atherosclerotic lesion area in the D + P + G group was significantly higher compared with the atherosclerotic lesion area in the D + P group ( $P=0.005$ , Figure 1A). In the thoracic (Figure 1B) and abdominal (Figure 1C) aortae, similar phenotypes were observed. When all lesions in the aortae (aortic arch, thoracic aorta, and abdominal aorta) were summed to calculate the whole proportion of atherosclerotic lesion, we found that pioglitazone treatment reduced atherosclerotic lesion area in ApoE<sup>-/-</sup> diabetic mice ( $p=0.003$ ), whereas the PPAR- $\gamma$  inhibitor GW9662 almost totally blocked this beneficial effect ( $p=0.015$ , Figure 1D).

### Pioglitazone treatment decreased the number of complicated atherosclerotic plaques in ApoE<sup>-/-</sup> diabetic mice

Complicated plaques were evaluated under H & E staining. As shown in Figure 2A and 2B, the number of complicated plaques in ApoE<sup>-/-</sup> diabetic mice (D group) was obviously higher than

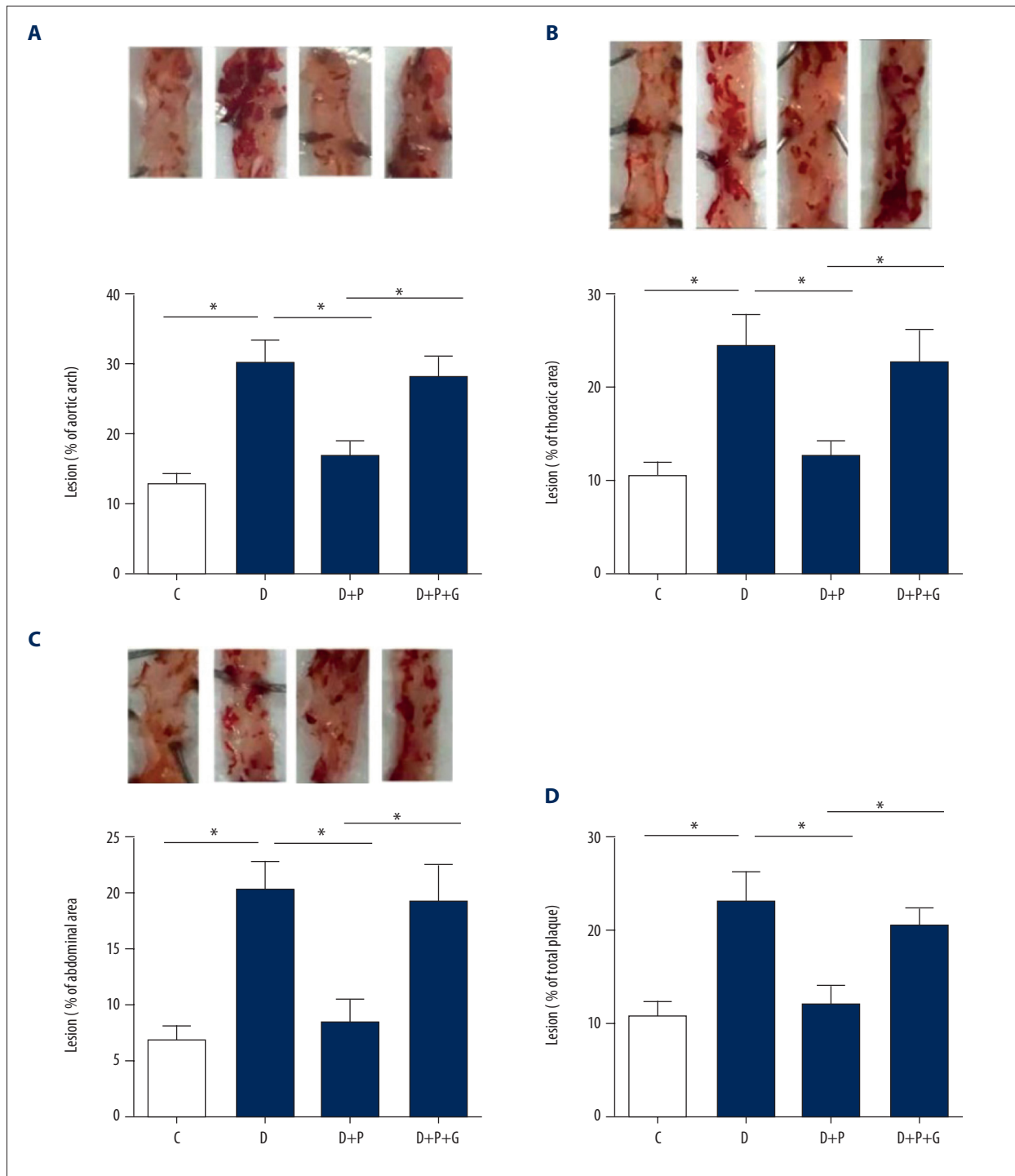


**Figure 1.** Effects of pioglitazone or pioglitazone + PPAR- $\gamma$  inhibitor GW9662 treatment on the atherosclerotic lesion area in ApoE<sup>-/-</sup> diabetic mice. (A–C) Representative Oil Red O staining images showing the atherosclerotic lesion area and quantitative analysis on the proportion of atherosclerotic lesions in aortic arch (A), thoracic aorta (B), and abdominal aorta (C) in ApoE<sup>-/-</sup> diabetic mice. \*  $p < 0.05$ .  $N = 8$  per group. (D) Quantitative analysis on the proportion of atherosclerotic lesions in whole aorta in ApoE<sup>-/-</sup> diabetic mice. \*  $p < 0.05$ .  $N = 8$  per group. C, control group; D, diabetic group; D + P, diabetic + pioglitazone group; D + P + G, diabetic + pioglitazone + GW9662 group.

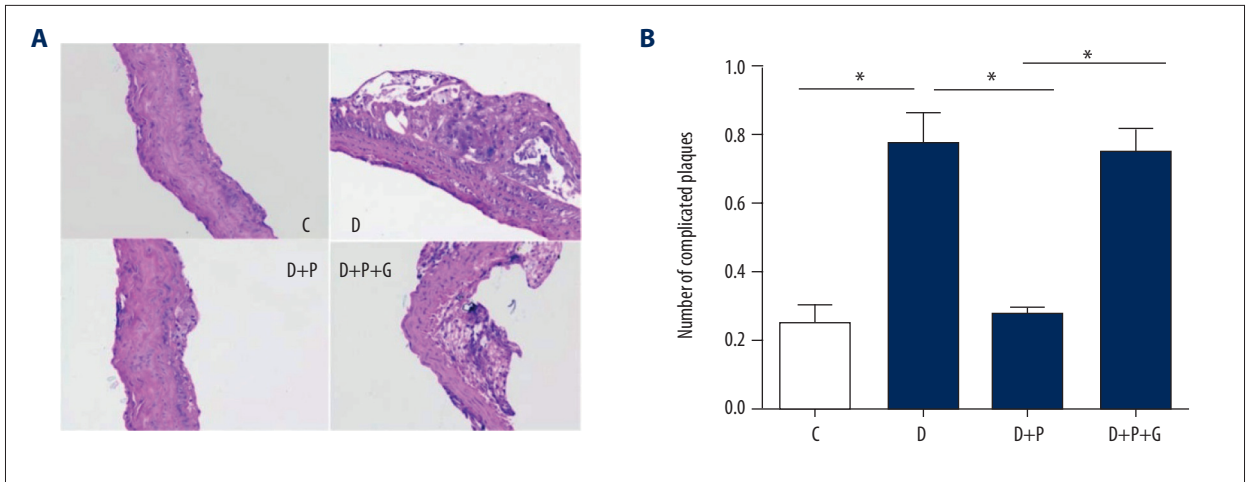


**Figure 2.** Effects of pioglitazone treatment on complicated atherosclerotic plaques in ApoE<sup>-/-</sup> diabetic mice. **(A)** Representative H&E staining images showing complicated atherosclerotic plaques. **(B)** Quantitative analysis of the number of complicated atherosclerotic plaques per visual field on microscopic examination. C – control group; D – diabetic group; D + P – diabetic + pioglitazone group; D + P + G – diabetic + pioglitazone + GW9662 group. \*  $p < 0.05$ .  $N = 8$  per group.

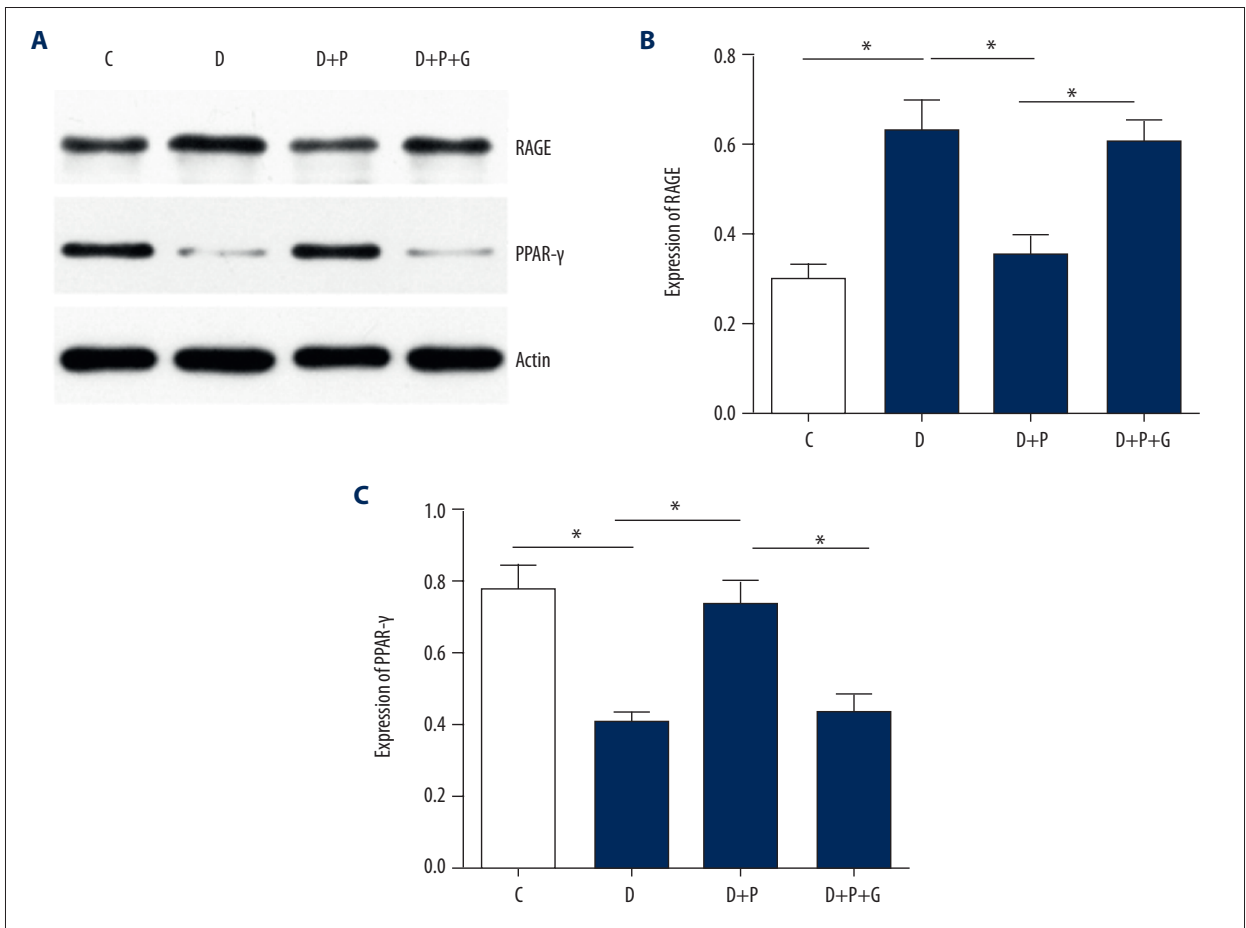


**Figure 3.** Effects of pioglitazone treatment on RAGE expression in atherosclerotic plaques of ApoE<sup>-/-</sup> diabetic mice by Western blotting analysis. Representative Western blotting images **(A)** and quantitative analysis of RAGE protein **(B)** and PPAR-γ protein **(C)** in atherosclerotic plaques. \*  $p < 0.05$ .  $N = 8$  per group.

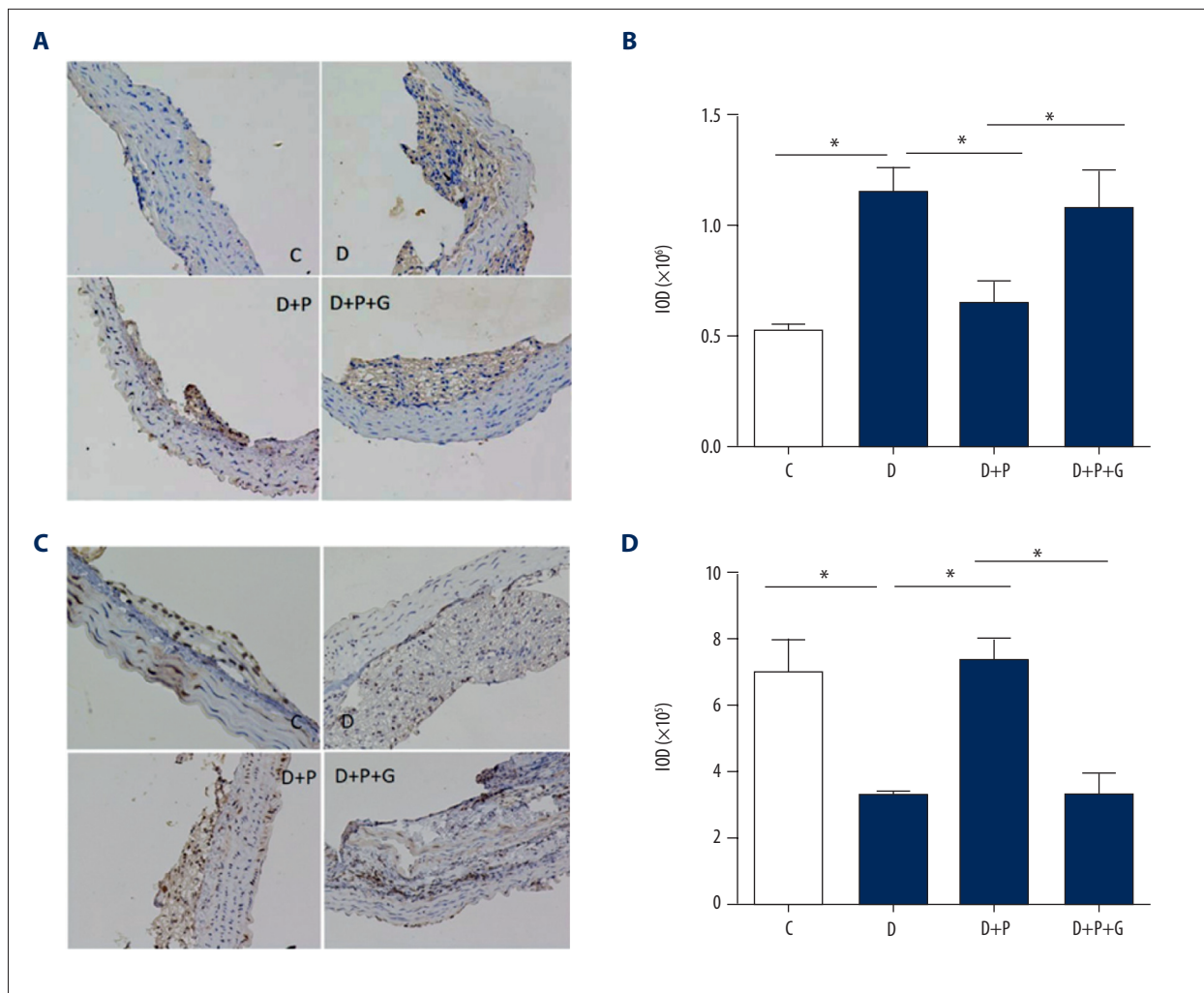


**Figure 4.** Effects of pioglitazone treatment on RAGE and PPAR- $\gamma$  expressions in atherosclerotic plaques of ApoE<sup>-/-</sup> diabetic mice by immunohistochemical analysis. Representative immunohistochemical staining images (A) and quantitative analysis (B) showing RAGE protein expression in atherosclerotic plaques. Representative immunohistochemical staining images (C) and quantitative analysis (D) showing PPAR- $\gamma$  protein expression in atherosclerotic plaques. C – control group; D – diabetic group; D + P – diabetic + pioglitazone group; D + P + G – diabetic + pioglitazone + GW9662 group. \*  $p < 0.05$ .  $N = 8$  per group.

that in ApoE<sup>-/-</sup> mice (C group,  $p = 0.001$ ). Pioglitazone treatment significantly reduced the number of complicated plaques in ApoE<sup>-/-</sup> diabetic mice ( $p = 0.001$ ), whereas a PPAR- $\gamma$  inhibitor GW9662 abolished this action ( $P = 0.002$ , Figure 2A, 2B).

#### Pioglitazone treatment suppressed RAGE expression while increasing PPAR- $\gamma$ expression in atherosclerotic lesions in ApoE<sup>-/-</sup> diabetic mice

The protein expressions of RAGE and PPAR- $\gamma$  were examined by Western blotting analysis. Compared with nondiabetic ApoE<sup>-/-</sup> mice (C group), ApoE<sup>-/-</sup> diabetic mice (D group) exhibited significantly increased expression of RAGE and decreased expression of PPAR- $\gamma$  in aortic tissue (both  $p = 0.001$ , Figure 3). Pioglitazone treatment remarkably reduced RAGE level, while

increasing PPAR- $\gamma$  level ( $p = 0.001$  and  $0.003$ , respectively); however, this effect was abolished by supplementation with a PPAR- $\gamma$  inhibitor GW9662 ( $p = 0.001$  and  $0.004$ , respectively).

Similar results were obtained by immunohistochemical analysis. The RAGE expression was remarkably increased (Figure 4A, 4B) while the PPAR- $\gamma$  expression (Figure 4C, 4D) was decreased in the atherosclerotic lesions of ApoE<sup>-/-</sup> diabetic mice (D group) compared with that in nondiabetic ApoE<sup>-/-</sup> mice (C group,  $p = 0.001$  and  $0.002$ , respectively). Pioglitazone treatment significantly reduced RAGE expression and enhanced PPAR- $\gamma$  expression in atherosclerotic plaques of diabetic mice (both  $p = 0.001$ ). Supplementation with GW9662 abolished the effect of pioglitazone on RAGE and PPAR- $\gamma$  expressions ( $p = 0.002$  and  $0.001$ , respectively; Figure 4B, 4D).

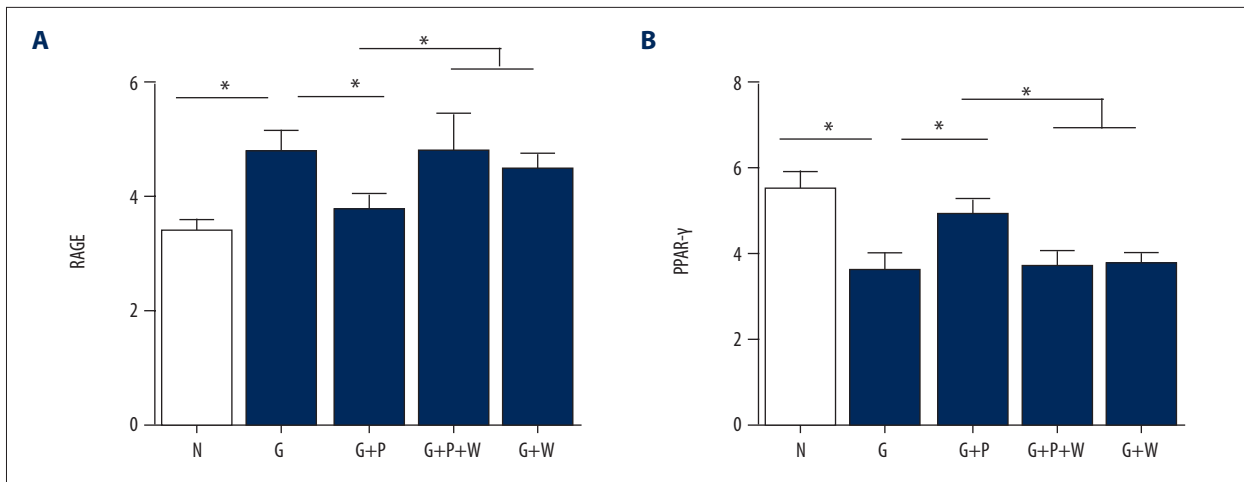


**Figure 5.** Effects of pioglitazone treatment on RAGE and PPAR- $\gamma$  mRNA expression in cultured primary mouse VSMCs. **(A)** Real-time PCR analysis showing mRNA expression of RAGE in VSMCs. **(B)** Real-time PCR analysis showing mRNA expression of PPAR- $\gamma$  in VSMCs. N – normal glucose; G – high glucose; P – pioglitazone; W – GW9662. \*  $p < 0.05$ . N=8 per group.

### Effects of pioglitazone on mRNA and protein expression of RAGE and PPAR- $\gamma$ in primary mouse VSMCs under high glycemic conditions

Next, we determined the effects of pioglitazone on RAGE and PPAR- $\gamma$  expression in primary mouse VSMCs. High-glucose enhanced RAGE (Figure 5A) but reduced PPAR- $\gamma$  mRNA expression (both  $p=0.001$ ; Figure 5B). Pioglitazone treatment partly inhibited the effects of high glucose on RAGE (Figure 5A) and PPAR- $\gamma$  (Figure 5B) mRNA expression in VSMCs,  $p=0.014$  and  $0.001$ , respectively. The PPAR- $\gamma$  inhibitor GW9662 abolished the effect of pioglitazone on RAGE and PPAR- $\gamma$  mRNA expression ( $p=0.001$  and  $0.002$ , respectively; Figure 5A, 5B). Interestingly, GW9662 administration had no effects on RAGE and PPAR- $\gamma$  mRNA expression in high-glucose conditions ( $p=0.946$  and  $0.964$ , respectively; Figure 5A, 5B, the last column vs. the second column). Further, we examined the protein expression of RAGE and PPAR- $\gamma$  (Figure 6A). Similarly, high glucose increased the RAGE but decreased PPAR- $\gamma$  protein expression ( $p=0.002$  and  $0.001$ , respectively), whereas pioglitazone treatment partly reversed the effects of high glucose on RAGE and PPAR- $\gamma$  protein expression ( $p=0.006$  and  $0.008$ , respectively; Figure 6B, 6C). Moreover, GW9662 blocked the effect of pioglitazone on RAGE and PPAR- $\gamma$  protein expression ( $p=0.004$  and  $0.012$ , respectively; Figure 6B, 6C).

## Discussion

In the present study, we investigated the effects of pioglitazone in diabetic ApoE<sup>-/-</sup> mice. The main findings of this study were: 1) administration of pioglitazone in diabetic ApoE<sup>-/-</sup> mice successfully inhibited progression of atherosclerosis; 2) pioglitazone inhibited RAGE mRNA and protein expression, both

in atherosclerotic plaques of diabetic ApoE<sup>-/-</sup> mice and cultured VSMCs, upon a high-glucose challenge; and 3) blockade of PPAR- $\gamma$  activity by the specific chemical inhibitor GW9662 remarkably attenuated the protective effects of pioglitazone against atherosclerosis in ApoE<sup>-/-</sup> mice and the inhibitory action of pioglitazone on RAGE mRNA and protein expression in cultured VSMCs upon high-glucose challenge. Taken together, these results demonstrate that pioglitazone, an oral antidiabetic agent, is able to attenuate atherosclerosis in diabetic mice *via* inhibiting RAGE signaling.

There exists a complex relationship between atherosclerosis and diabetes. Atherosclerosis can be considered one of the most important causes of cardiovascular disease in the diabetic population, and diabetes further aggravates atherosclerosis to increase the risk of cardiovascular events [1,2]. Hyperglycemia-induced inflammation in the vasculature has been reported to be the most important cause of atherogenesis [5]. Moreover, other molecular mechanisms, including the proliferation of VSMCs, endothelial injury, activation of vascular inflammation, augmentation of reactive oxygen species (ROS), dysregulation of the renin-angiotensin system (RAS), impaired insulin sensitivity, and altered production of adipocytokines, chronically perturb the vasculature and lead to increased numbers, size, and complexity of atherosclerotic plaques under diabetic conditions [27,28]. Interestingly, the antidiabetic agent pioglitazone has an effect on atherosclerosis. Game et al. reported that pioglitazone significantly inhibited the high-fat-diet- and TGF- $\alpha$ -induced expression of connective tissue growth factor in mouse advanced atherosclerotic plaques and in cultured human VSMCs, respectively [29]. Joner et al. found a 21% reduction in neointimal area for high-dose pioglitazone-treated atherosclerotic rabbits, which was associated with a significant reduction of neointimal macrophages [30]. Several recent animal studies have confirmed the protective effect of



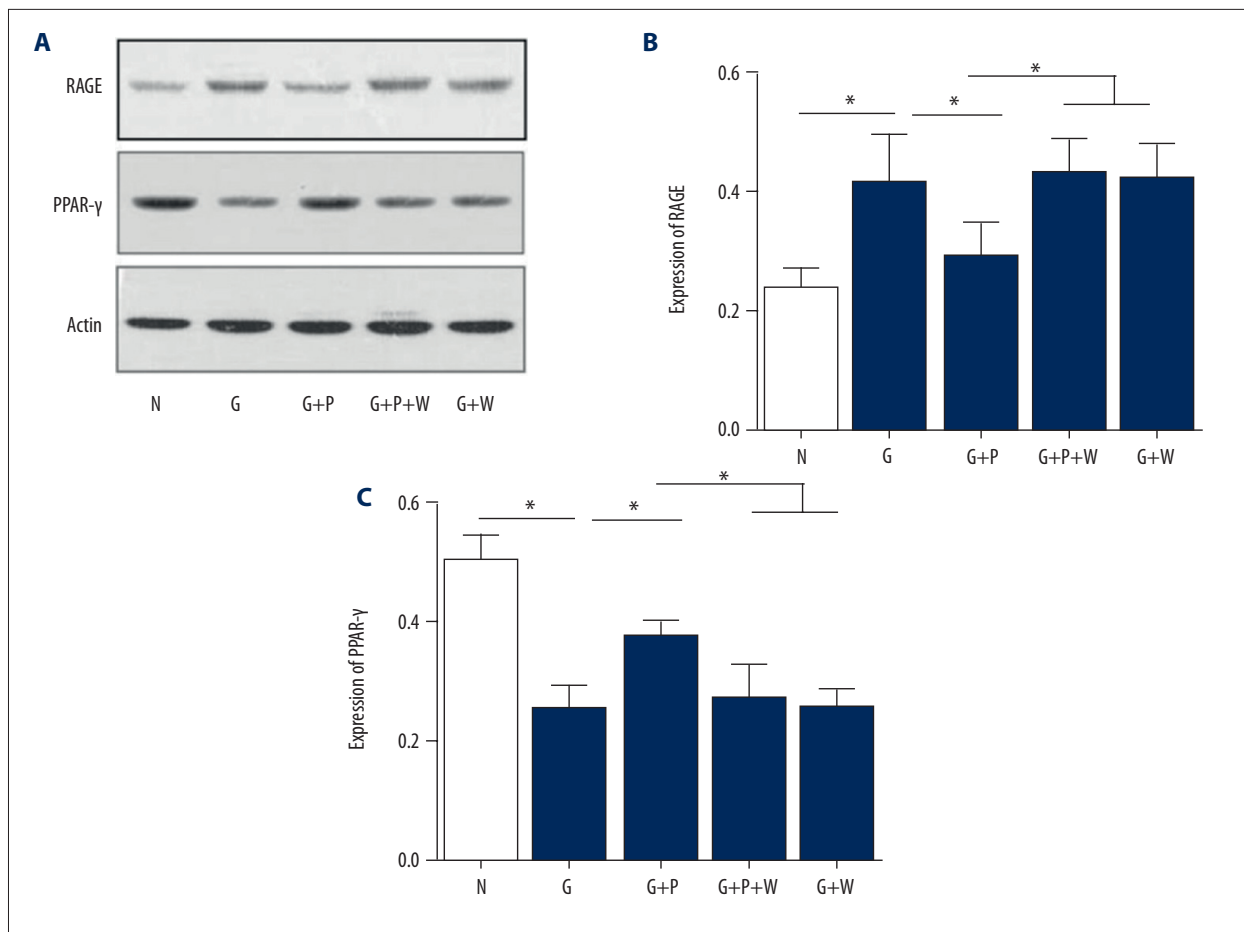


**Figure 6.** Effects of pioglitazone treatment on RAGE and PPAR- $\gamma$  protein expression in cultured primary mouse VSMCs. (A) Representative Western blotting images showing RAGE and PPAR- $\gamma$  protein expression in VSMCs. Actin was used to as a loading control. (B, C) Quantitative analysis of RAGE (B) and PPAR- $\gamma$  (C) protein expression in VSMCs. N – normal glucose; G – high glucose; P – pioglitazone; W – GW9662. \*  $p < 0.05$ . N=8 per group.

pioglitazone against atherosclerosis [31,32]. Furthermore, many large-scale clinical investigations have supported the beneficial action of pioglitazone on atherosclerosis prevention and treatment [11–13]. However, there are some conflicting reports. An investigation showed that pioglitazone administration substantially increased apoptotic cells and plaque necrosis in low-density lipoprotein receptor (LDLR) knockout mice fed a non-diabetogenic cholesterol-enriched diet [33], suggesting that pioglitazone may have adverse effects on advanced atherosclerosis by promoting plaque instability. Activation of PPAR- $\gamma$  seemed to promote monocyte/macrophage differentiation and uptake of oxidized LDL [34]. Therefore, this issue remains controversial and the direct evidence of the effect of pioglitazone in the development of diabetic atherosclerosis is lacking. In our study, pioglitazone not only reduced the size of the atherosclerotic lesion, but also significantly decreased the number of complicated atherosclerotic plaques in ApoE<sup>-/-</sup> diabetic mice. Thus, our results support the favorable effect of pioglitazone in the prevention or treatment of atherosclerosis.

Another important feature of our study is that we provide here the first evidence that the inhibition of RAGE signaling by pioglitazone contributes to its protection against atherosclerosis in diabetes. Although great efforts have been made to identify the underlying mechanisms for aggravation of atherosclerosis under diabetic conditions, our understanding on this issue is not complete. As an insulin-sensitizer, pioglitazone was reported to reduce the escape latency in the Morris water maze test and improve cognition function by decreasing RAGE expression in the cerebral cortex of fructose-drinking rats [35]. Moreover, pioglitazone significantly reversed the impairment of learning and memory behavior *via* RAGE inhibition in the brain in an STZ-induced diabetic mouse model [36]. Intriguingly, RAGE expression is closely associated with pathological staging and tumor invasion of human hepatocellular carcinoma, and pioglitazone inhibits growth and invasion of human hepatocellular carcinoma *via* blockade of RAGE signaling [37]. These results indicate that RAGE signaling may be a target of pioglitazone. Our results clearly show that RAGE protein

expression in atherosclerosis plaque was reduced by pioglitazone. In addition, our *in vitro* results confirmed this phenotype by showing that pioglitazone decreased both mRNA and protein expression of RAGE in cultured VSMCs. Further, we explored how pioglitazone downregulates RAGE expression in VSMCs. Blockade of PPAR- $\gamma$  by a selective inhibitor, GW9662, not only totally abolished the protective effects of pioglitazone against atherosclerosis in ApoE<sup>-/-</sup> mice, but also revoked the inhibitory effects of pioglitazone on RAGE mRNA and protein expression. These results strongly suggest that pioglitazone attenuates atherogenesis and suppresses RAGE signaling in a PPAR- $\gamma$ -dependent manner, which are consistent with previous evidence that pioglitazone downregulated RAGE expression and inhibited ROS production and NF- $\kappa$ B activation in coronary artery smooth muscle cells *via* PPAR- $\gamma$  activation [38].

## References:

- Kannel WB, McGee DL: Diabetes and cardiovascular disease. The Framingham study. *JAMA*, 1979; 241: 2035–38
- Gu K, Cowie CC, Harris MI: Diabetes and decline in heart disease mortality in US adults. *JAMA*, 1999; 281: 1291–97
- Gaede P, Vedel P, Larsen N et al: Multifactorial intervention and cardiovascular disease in patients with type 2 diabetes. *N Engl J Med*, 2003; 348: 383–93
- Beckman JA, Creager MA, Libby P: Diabetes and atherosclerosis: Epidemiology, pathophysiology, and management. *JAMA*, 2002; 287: 2570–81
- Low WC, Hess CN, Hiatt WR, Goldfine AB: Clinical update: Cardiovascular disease in diabetes mellitus: Atherosclerotic cardiovascular disease and heart failure in type 2 diabetes mellitus – mechanisms, management, and clinical considerations. *Circulation*, 2016; 133: 2459–502
- Bucciarelli LG, Wendt T, Qu W et al: RAGE blockade stabilizes established atherosclerosis in diabetic apolipoprotein E-null mice. *Circulation*, 2002; 106: 2827–35
- Xiao CC, Ren A, Yang J et al: Effects of pioglitazone and glipizide on platelet function in patients with type 2 diabetes. *Eur Rev Med Pharmacol Sci*, 2015; 19: 963–70
- Nitta Y, Tahara N, Tahara A et al: Pioglitazone decreases coronary artery inflammation in impaired glucose tolerance and diabetes mellitus: Evaluation by FDG-PET/CT imaging. *JACC Cardiovasc Imaging*, 2013; 6: 1172–82
- van der Meer RW, Rijzewijk LJ, de Jong HW et al: Pioglitazone improves cardiac function and alters myocardial substrate metabolism without affecting cardiac triglyceride accumulation and high-energy phosphate metabolism in patients with well-controlled type 2 diabetes mellitus. *Circulation*, 2009; 119: 2069–77
- Lee M, Saver JL, Liao HW et al: Pioglitazone for secondary stroke prevention: A systematic review and Meta-Analysis. *Stroke*, 2017; 48: 388–93
- Nicholls SJ, Tuzcu EM, Wolski K et al: Lowering the triglyceride/high-density lipoprotein cholesterol ratio is associated with the beneficial impact of pioglitazone on progression of coronary atherosclerosis in diabetic patients: Insights from the PERISCOPE (Pioglitazone Effect on Regression of Intravascular Sonographic Coronary Obstruction Prospective Evaluation) study. *J Am Coll Cardiol*, 2011; 57: 153–59
- Mizoguchi M, Tahara N, Tahara A et al: Pioglitazone attenuates atherosclerotic plaque inflammation in patients with impaired glucose tolerance or diabetes a prospective, randomized, comparator-controlled study using serial FDG PET/CT imaging study of carotid artery and ascending aorta. *JACC Cardiovasc Imaging*, 2011; 4: 1110–18
- Mani P, Uno K, St JJ et al: Favorable impact on LDL particle size in response to treatment with pioglitazone is associated with less progression of coronary atherosclerosis in patients with type 2 diabetes. *J Am Coll Cardiol*, 2015; 66: 328–29
- Gao XJ, Qu YY, Liu XW et al: Immune complexes induce TNF- $\alpha$  and BAFF production from U937 cells by HMGB1 and RAGE. *Eur Rev Med Pharmacol Sci*, 2017; 21: 1810–19
- Hofmann MA, Drury S, Fu C et al: RAGE mediates a novel proinflammatory axis: A central cell surface receptor for S100/calgranulin polypeptides. *Cell*, 1999; 97: 889–901
- Farmer DG, Kennedy S: RAGE, vascular tone and vascular disease. *Pharmacol Ther*, 2009; 124: 185–94
- Cipollone F, Iezzi A, Fazio M et al: The receptor RAGE as a progression factor amplifying arachidonate-dependent inflammatory and proteolytic response in human atherosclerotic plaques: Role of glycemic control. *Circulation*, 2003; 108: 1070–77
- Cantero AV, Portero-Otin M, Ayala V et al: Methylglyoxal induces advanced glycation end product (AGEs) formation and dysfunction of PDGF receptor-beta: Implications for diabetic atherosclerosis. *Faseb J*, 2007; 21: 3096–106
- Pan JH, Sukhova GK, Yang JT et al: Macrophage migration inhibitory factor deficiency impairs atherosclerosis in low-density lipoprotein receptor-deficient mice. *Circulation*, 2004; 109: 3149–53
- Wang P, Xu TY, Guan YF et al: Vascular smooth muscle cell apoptosis is an early trigger for hypothyroid atherosclerosis. *Cardiovasc Res*, 2014; 102: 448–59
- Wang P, Xu TY, Guan YF et al: Nicotinamide phosphoribosyltransferase protects against ischemic stroke through SIRT1-dependent adenosine monophosphate-activated kinase pathway. *Ann Neurol*, 2011; 69: 360–74
- Speidl WS, Cimmino G, Ibanez B et al: Recombinant apolipoprotein A-I Milano rapidly reverses aortic valve stenosis and decreases leaflet inflammation in an experimental rabbit model. *Eur Heart J*, 2010; 31: 2049–57
- Golovina VA, Blaustein MP: Preparation of primary cultured mesenteric artery smooth muscle cells for fluorescent imaging and physiological studies. *Nat Protoc*, 2006; 1: 2681–87
- Wang P, Xu TY, Guan YF et al: Perivascular adipose tissue-derived visfatin is a vascular smooth muscle cell growth factor: Role of nicotinamide mononucleotide. *Cardiovasc Res*, 2009; 81: 370–80
- Wang P, Xu TY, Wei K et al: ARRB1/beta-arrestin-1 mediates neuroprotection through coordination of BECN1-dependent autophagy in cerebral ischemia. *Autophagy*, 2014; 10: 1535–48
- Wang P, Guan YF, Du H et al: Induction of autophagy contributes to the neuroprotection of nicotinamide phosphoribosyltransferase in cerebral ischemia. *Autophagy*, 2012; 8: 77–87
- Wang P, Du H, Zhou CC et al: Intracellular NAMPT-NAD<sup>+</sup>-SIRT1 cascade improves post-ischaemic vascular repair by modulating Notch signalling in endothelial progenitors. *Cardiovasc Res*, 2014; 104: 477–88
- Zhao Y, Guan YF, Zhou XM et al: Regenerative neurogenesis after ischemic stroke promoted by nicotinamide Phosphoribosyltransferase-Nicotinamide adenine dinucleotide cascade. *Stroke*, 2015; 46: 1966–74
- Game BA, He L, Jarido V et al: Pioglitazone inhibits connective tissue growth factor expression in advanced atherosclerotic plaques in low-density lipoprotein receptor-deficient mice. *Atherosclerosis*, 2007; 192: 85–91

## Conclusions

Our results demonstrate that administration of pioglitazone in diabetic ApoE<sup>-/-</sup> mice successfully inhibited development of atherosclerosis through inhibiting RAGE signaling in a PPAR- $\gamma$ -dependent manner. These results support the therapeutic effect of pioglitazone on atherosclerosis in diabetes, and show the critical role of inhibition of RAGE signaling for the beneficial effects of pioglitazone.

## Conflict of Interest

None.

30. Joner M, Farb A, Cheng Q et al: Pioglitazone inhibits in-stent restenosis in atherosclerotic rabbits by targeting transforming growth factor-beta and MCP-1. *Arterioscler Thromb Vasc Biol*, 2007; 27: 182–89
31. Subramanian V, Golledge J, Ijaz T et al: Pioglitazone-induced reductions in atherosclerosis occur via smooth muscle cell-specific interaction with PPAR{gamma}. *Circ Res*, 2010; 107: 953–58
32. Nakashiro S, Matoba T, Umezu R et al: Pioglitazone-Incorporated nanoparticles prevent plaque destabilization and rupture by regulating Monocyte/Macrophage differentiation in ApoE<sup>-/-</sup> mice. *Arterioscler Thromb Vasc Biol*, 2016; 36: 491–500
33. Thorp E, Kuriakose G, Shah YM et al: Pioglitazone increases macrophage apoptosis and plaque necrosis in advanced atherosclerotic lesions of non-diabetic low-density lipoprotein receptor-null mice. *Circulation*, 2007; 116: 2182–90
34. Tontonoz P, Nagy L, Alvarez JG et al: PPARgamma promotes monocyte/macrophage differentiation and uptake of oxidized LDL. *Cell*, 1998; 93: 241–52
35. Liu X, Luo D, Zheng M et al: Effect of pioglitazone on insulin resistance in fructose-drinking rats correlates with AGEs/RAGE inhibition and block of NADPH oxidase and NF kappa B activation. *Eur J Pharmacol*, 2010; 629: 153–58
36. Xiao CC, Ren A, Yang J et al: Effects of pioglitazone and glipizide on platelet function in patients with type 2 diabetes. *Eur Rev Med Pharmacol Sci*, 2015; 19: 963–70
37. Yang Y, Zhao LH, Huang B et al: Pioglitazone, a PPARgamma agonist, inhibits growth and invasion of human hepatocellular carcinoma via blockade of the rage signaling. *Mol Carcinog*, 2015; 54: 1584–95
38. Di BB, Li HW, Li WP et al: Pioglitazone inhibits high glucose-induced expression of receptor for advanced glycation end products in coronary artery smooth muscle cells. *Mol Med Rep*, 2015; 11: 2601–7